

Determination of the Secondary Structure and Molecular Topology of Interleukin-1 β by Use of Two- and Three-Dimensional Heteronuclear ^{15}N - ^1H NMR Spectroscopy[†]

Paul C. Driscoll,[†] Angela M. Gronenborn,^{*,†} Paul T. Wingfield,[§] and G. Marius Clore^{*,†}

Laboratory of Chemical Physics, Building 2, National Institute of Diabetes, Digestive and Kidney Diseases, National Institutes of Health, Bethesda, Maryland 20892, and Glaxo Institute for Molecular Biology SA, 46 Rue des Acacias, CH-1211 Geneva, Switzerland

Received November 22, 1989; Revised Manuscript Received January 26, 1990

ABSTRACT: A study of the regular secondary structure elements of recombinant human interleukin-1 β has been carried out using NMR spectroscopy. Using a randomly ^{15}N labeled sample, a number of heteronuclear three- and two-dimensional NMR experiments have been performed, which have enabled a complete analysis of short-, medium-, and long-range NOEs between protons of the polypeptide backbone, based on the sequence-specific resonance assignments that have been reported previously [Driscoll, P. C., Clore, G. M., Marion, D., Wingfield, P. T., & Gronenborn, A. M. (1990) *Biochemistry* 29, 3542–3556]. In addition, accurate measurements of a large number of $^3J_{\text{HN}\alpha}$ coupling constants have been carried out by two-dimensional heteronuclear multiple-quantum-coherence- J spectroscopy. Amide NH solvent exchange rates have been measured by following the time dependence of the ^{15}N - ^1H correlation spectrum of interleukin-1 β on dissolving the protein in D_2O solution. Analysis of these data indicate that the structure of interleukin-1 β consists of 12 extended β -strands aligned in a single extended network of antiparallel β -sheet structure that in part folds into a skewed six-stranded β -barrel. In the overall structure the β -strands are connected by tight turns, short loops, and long loops in a manner that displays approximate pseudo-three-fold symmetry. The secondary structure analysis is discussed in the light of the unrefined X-ray structure of interleukin-1 β at 3-Å resolution [Priestle, J. P., Schär, H.-P., & Grütter, M. G. (1988) *EMBO J.* 7, 339–343], as well as biological activity data. Discernible differences between the two studies are highlighted. Finally, we have discovered conformational heterogeneity in the structure of interleukin-1 β , which is characterized by an exchange rate that is slow on the NMR chemical shift time scale.

Interleukin-1 β (IL-1 β)¹ is a monocyte-derived cytokine protein that plays a central role in the immune and inflammatory responses. A number of specific biological activities have been identified for the mature form of this protein, which comprises 153 amino acid residues and has a molecular mass of 17.4 kDa. These include stimulation of B-lymphocyte proliferation, induction of acute-phase protein synthesis by hepatocytes, fibroblast growth factor activity, and thymocyte proliferation via the induction of interleukin-2 release [see Dinarello (1984, 1988), Oppenheim et al. (1986), and Moore (1989) for reviews]. Many of these activities are shared with a related protein called interleukin-1 α , which exhibits 25% sequence homology with IL-1 β (Auron et al., 1984; March et al., 1985). We have been engaged in a study of structure-function relationships for both proteins using NMR spectroscopy and site-directed mutagenesis (Gronenborn et al., 1986, 1988; MacDonald et al., 1986; Wingfield et al., 1987a–c, 1989). One goal of these studies is to obtain the three-dimensional solution structure of IL-1 β on the basis of interproton distance restraints derived from nuclear Overhauser effect (NOE) data (Wüthrich, 1986; Clore & Gronenborn, 1987, 1989). The structures of a number of proteins of less

than ca. 100 amino acid residues have been obtained by two-dimensional (2D) ^1H NMR spectroscopy. However, the successful application of these methods to a protein the size of IL-1 β remains a significant challenge. There are two main reasons for this difficulty. First, the increased complexity of the ^1H spectrum leads to a higher degree of chemical shift degeneracy in the 2D spectra, which in turn makes unambiguous identification of all signals in the NOESY spectrum more difficult, if not impossible. Second, increased overall correlation times lead to greater resonance line widths and much reduced efficiency of magnetization transfer between scalar-coupled protons, making spin system identification more difficult.

A great deal of effort is now being applied to solving these problems. New strategies of NMR spectrum analysis based on ^{15}N and ^{13}C labeling of proteins are being successfully applied to “larger” recombinant proteins such as T4 lysozyme (McIntosh et al., 1987a,b), staphylococcal nuclease (Torchia et al., 1988, 1989), flavodoxin (Stockman et al., 1988), human thioredoxin (Forman-Kay et al., 1989), Mu ner (Gronenborn et al., 1989c), interleukin-1 β (Marion et al., 1989b; Driscoll et al., 1990), and calmodulin (Ikura et al., 1990). Initial strategies were based on the selective labeling of specific types

[†] This work was supported by the Intramural AIDS targeted Antiviral Program of the Office of the Director of the National Institutes of Health (to G.M.C. and A.M.G.).

[‡] National Institute of Diabetes, Digestive and Kidney Diseases.

[§] Glaxo Institute for Molecular Biology SA. Present address: Protein Expression Laboratory, National Institutes of Health, Bethesda, MD 20892.

¹ Abbreviations used: IL-1, interleukin-1; IL-1 α , interleukin-1 α ; IL-1 β , interleukin-1 β ; NMR, nuclear magnetic resonance; NOE, nuclear Overhauser effect; NOESY, nuclear Overhauser effect spectroscopy; HOHAHA, homonuclear Hartmann–Hahn spectroscopy; HMQC, heteronuclear multiple-quantum-coherence spectroscopy; COSY, correlated spectroscopy; P.COSY, primitive COSY.

of amino acid within the protein combined with 2D heteronuclear NMR spectroscopy [see McIntosh and Dahlquist (1990) for review]. More recent approaches, on the other hand, have made use of uniform random labeling with a heteronucleus in combination with 2D and 3D heteronuclear spectroscopic methods (Oh et al., 1988; Clore et al., 1988; Gronenborn et al., 1989a; Kay et al., 1989a). Perhaps the most promising and widely applicable experiments are those using 3D heteronuclear spectroscopy of uniformly labeled proteins (Zuiderweg & Fesik, 1989; Marion et al., 1989b). In general, these experiments provide 3D spectra in which a 2D ^1H NOESY, COSY, or HOHAHA spectrum is resolved with respect to the chemical shifts of the directly bonded heteronuclei. Recently we reported the complete assignment of the backbone amide NH and C^αH resonances of IL-1 β (Driscoll et al., 1990). The assignments were obtained by using primarily 3D ^1H - ^1H NOESY- ^{15}N - ^1H HMQC and 3D ^1H - ^1H HOHAHA- ^{15}N - ^1H HMQC spectroscopy of a uniformly ^{15}N labeled sample (Marion et al., 1989a,b). Almost complete resolution of the NH region and the 2D ^1H NOESY and HOHAHA spectra was obtained by these methods, which allowed a relatively straightforward analysis for the sequence-specific assignment. The same spectra also proved useful for the identification of medium- and long-range backbone NOEs that can be used in the analysis of secondary structure.

As a preliminary phase in the complete process of determining a solution structure of a protein by NMR methods, it is useful to delineate the elements of secondary structure in the protein. This procedure is important as it can lead to the resolution of ambiguous NOEs during the sequence-specific assignment and aids the complete analysis of the long-range tertiary NOEs that are required for full structure calculations. The identification of secondary structure elements can be performed on the basis of a number of readily identifiable NMR parameters associated with the backbone resonances alone. In this paper we report the elucidation of the secondary structure of this protein based on the NMR assignments, short-, medium-, and long-range NOEs, NH- C^αH coupling constants, and amide NH solvent-exchange rates. We show that IL-1 β contains a very high degree of antiparallel β -sheet structure, which is connected by reverse turns and long loops. There is no evidence for any helical elements. The results of this analysis are discussed in the light of the unrefined 3 Å resolution X-ray structure of IL-1 β (Priestle et al., 1988).²

EXPERIMENTAL PROCEDURES

Preparation of IL-1 β . The preparation and purification of recombinant wild type, des-[Ala-1], and mutant (K27C, K93A, and K94A) IL-1 β proteins was as described previously (Wingfield et al., 1986; Gronenborn et al., 1986; Driscoll et al., 1990). Uniform ^{15}N labeling (>95%) of the wild type and des-[Ala-1] IL-1 β proteins was performed by growing the cells in minimal medium with $^{15}\text{NH}_4\text{Cl}$ as the sole nitrogen source. The buffer used for the preparation of samples for NMR spectroscopy was 100 mM sodium acetate- d_3 (95% H_2O /

5% D_2O), pH 5.4. Samples for spectra recorded in D_2O solution were freeze-dried from this buffer and dissolved in 99.995% D_2O . The protein concentration used was in the range of 2.0–2.3 mM.

NMR Spectroscopy. All NMR experiments were recorded on a Bruker AM600 spectrometer, operating in "reverse" mode. The assignment of long-range NOEs was based in part on the following ^1H 2D experiments applied to wild type, des-[Ala-1], and mutant IL-1 β samples in H_2O solution: 100-ms NOESY (Jeener et al., 1979; Macura et al., 1981), 30-ms HOHAHA (Braunschweiler & Ernst, 1983; Davis & Bax, 1985), and COSY (Aue et al., 1976). The NOESY and HOHAHA experiments were recorded by using a jump and return "read" pulse to suppress the solvent resonance (Bax et al., 1987; Driscoll et al., 1989). The COSY spectra were recorded by using phase-locked low-power presaturation of the H_2O signal combined with the SCUBA pulse sequence for the recovery of C^αH signals that are coincident with the solvent resonance (Brown et al., 1987). For the identification of long-range C^αH - C^αH NOEs in the aliphatic region of the spectrum, a series of spectra were recorded for the wild type and K27C IL-1 β proteins in D_2O solution, including 100-ms NOESY, 30-ms HOHAHA, and P.COSY spectra (Mueller 1987; Marion & Bax, 1988). Phase-locked low-power presaturation of the residual HOD resonance was utilized in all the D_2O experiments. For the wild-type protein these spectra were recorded at 27 and 36 °C. For all other samples the temperature used was 36 °C. A sweep width of 8.0–8.4 kHz was used in each dimension, with typically 800–900 t_1 increments each of 2K data points in the F_2 dimension. Quadrature detection in the F_1 dimension was obtained by using time proportional phase incrementation (Ernst et al., 1987) in the phase-sensitive mode as described by Marion and Wüthrich (1983). HOHAHA experiments utilized a WALTZ-17 mixing pulse sequence (Bax, 1989) in combination with a delay period for the compensation of rotating frame NOE effects.

A number of experiments were recorded to investigate the conformational exchange present in the samples of IL-1 β , as manifested by exchange cross-peaks in the amide region of the ^1H 2D HOHAHA and NOESY spectra. These included a series of 2D ^1H spin-lock experiments in which the transmitter was placed downfield of the amide NH region of the spectrum. A weak WALTZ-17 spin-lock field (90° pulse = 45 μs) was used for the mixing period with durations of 20, 40, and 80 ms. The 17th pulse of the WALTZ spin-lock pulse train was set to 180°.

The 3D ^1H - ^1H NOESY- ^{15}N - ^1H HMQC (3D NOESY-HMQC) and 3D ^1H - ^1H HOHAHA- ^{15}N - ^1H HMQC (3D HOHAHA-HMQC) experiments used in the analysis of long-range NOEs in the NH-NH/aromatic and NH-aliphatic regions of the H_2O spectrum of wild-type IL-1 β are exactly those experiments that were used for the sequence-specific assignment, which we reported earlier (Driscoll et al., 1990). For a full description of the pulse sequences and parameters for these heteronuclear 3D experiments, the reader is referred to our previous publications (Marion et al., 1989b; Driscoll et al., 1990). Data processing of the 3D experiments was carried out as described by Kay et al. (1989a).

$^3J_{\text{NH}\alpha}$ Coupling Constants. Accurate measurements of $^3J_{\text{NH}\alpha}$ coupling constants were obtained by using the HMQC- J pulse sequence (Kay & Bax, 1990). The experiment was performed with both the wild-type and des-[Ala-1] IL-1 β samples in H_2O at 36 °C. However, superior results were obtained for the des-[Ala-1] IL-1 β sample because of its greater chemical homogeneity (see Results and Discussion).

² Added in proof: Since the submission and acceptance of this paper, two papers on the refined X-ray structure of IL-1 β at 2-Å resolution have appeared in the literature (Finzel et al., 1989; Priestle et al., 1989). The results of the secondary structure analysis reported in this paper are now in complete agreement with the high-resolution X-ray data (Finzel et al., 1989), and the disagreement for the location of the turn between strands VIII and IX between the NMR data (residues 106–109) and the unrefined 3-Å resolution structure of Priestle et al. (1988) (residues 104–107) is now resolved in favor of the NMR analysis.

The experiment was recorded with 2K data points in F_2 and a sweep width of 4.17 kHz, with the carrier set in the center of the amide NH region of the spectrum and the H_2O signal located at the right-hand edge of the spectrum. A total of 702 increments were recorded in the ^{15}N dimension with a sweep width of 1.67 kHz, yielding a total 210.6 ms t_1 acquisition time. The H_2O resonance was suppressed by use of a DANTE-style pulse train, which provides off-resonance decoupling (Kay et al., 1989a). Zero-filling to 4K data points was applied in the F_1 dimension to yield a final digital resolution of 0.41 Hz/point. The spectrum was processed three times by using different negative line broadening parameters (-6, -8, and -10 Hz) for the Lorentz-to-Gaussian apodization function in the F_1 dimension with the maximum of the window function set at the end of the t_1 time domain data. Apparent $^3J_{NH\alpha}$ values were measured from the cross-peak splittings in the ^{15}N dimension in each version of the processed spectrum. These apparent J splittings include contributions arising from the slight dispersive character of the line shape in F_1 and the multiplet component overlap due to finite line width. Corrected values of $^3J_{NH\alpha}$ coupling constants were then obtained by a nonlinear least-squares optimization of the difference between the splittings obtained from simulated line shapes with those obtained experimentally, with the multiple-quantum line width and $^3J_{NH\alpha}$ as variable parameters (Forman-Kay et al., 1990). The data were fitted by using an initial guess for $^3J_{NH\alpha}$ equal to the experimentally measured splitting and three initial values for the multiple-quantum line width: 10, 12, and 13 Hz. The final corrected coupling constants are accurate to ± 0.5 Hz.

NH Exchange Rates. Amide NH solvent exchange rates were measured by following the intensity of cross-peaks in a 1H -detected ^{15}N - 1H correlation experiment as a function of time. The pulse sequence used incorporates a double INEPT transfer of magnetization from 1H to ^{15}N and back again, commonly known as the "Overbodenhausen" experiment (Bodenhausen & Ruben, 1980; Bax et al., 1990; Marion et al., 1989c). The pulse sequence for this experiment is given by

1H : $90_x-\Delta-180_x-\Delta-90_y-t_1/2-90_x-240_y-90_x-t_1/2-90_x-\Delta-180_x-\Delta-Acq-\chi$
 ^{15}N : $180_x-90_\phi-90_\psi-180_x-Decouple$

The delay Δ is set to 2.3 ms, slightly shorter than $1/(4J_{NH})$. The pulse in the center of the evolution period is a composite 180° 1H pulse. Time proportional phase incrementation is applied to phase ϕ to achieve quadrature detection in F_1 . The minimum phase cycle we have used is $\phi = x, -x$; $\chi = x, -x$; $\psi = x$. This suppresses signals due to protons not directly bound to the ^{15}N heteronucleus. Reasonable spectra could be acquired with two scans per t_1 increment by using this phase cycle. Longer experiments were based on the following four-step phase cycle: $\phi = x, -x, -x, x$; $\chi = x, -x, x, -x$; $\psi = x, x, -x, -x$. ^{15}N decoupling in F_2 was carried out on a "hard-wired" decoupler unit utilizing GARP (Shaka et al., 1985) phase modulation.

Using uniformly ^{15}N labeled protein and an Overbodenhausen experiment, in which the vast majority of the amide resonances are resolved, provides an excellent method for the simultaneous measurement of the exchange rates of all the slowly exchanging amide NHs (Marion et al., 1989c). On our modified Bruker AM600 spectrometer we are able to obtain such a spectrum of a 2 mM ^{15}N -labeled sample with good sensitivity in as little time as 10 min. It is therefore possible to achieve both good time and spectral resolution with this type of experiment. A sample of wild-type IL-1 β was prepared in

H_2O solution containing 100 mM sodium acetate- d_3 , pH 5.4, and freeze-dried (this causes a pH change to 6.1, as measured at the end of the exchange experiment). To start the NH solvent exchange measurement, 99.8% D_2O was added to the freeze-dried protein sample at 0 $^\circ C$. The sample was inserted in the magnet at 36 $^\circ C$ and allowed to come to thermal equilibrium, as judged by the stability of the deuterium lock signal. The first Overbodenhausen experiment was started 5 min after the addition of D_2O to the sample. A series of 2D Overbodenhausen experiments were then recorded over a period of nearly 2 days. The sweep width used in F_2 was 4.17 kHz, with the carrier set to the center of the amide NH region of the spectrum with the residual HOD signal on the right-hand edge. Very low power DANTE-style off-resonance irradiation was used to suppress the residual solvent signal (Kay et al., 1989a). A total of 256 t_1 increments, each of 2K data points, were recorded, giving a total acquisition time of 66.6 ms and a sweep width of 1.92 kHz in the F_1 dimension. These experiments were recorded in a manner that is a little out of the ordinary. Instead of recording all steps of the phase cycle before incrementing the t_1 evolution time, we recorded all t_1 increments for each step of the phase cycle before stepping through the phase cycle. This avoids the use of unnecessarily time consuming dummy scans for each t_1 increment. Instead, we employ a simple scheme at the beginning of each step of the phase cycle that brings the system to a steady state (Marion et al., 1989c). In total, 10 experiments were recorded at the following times after the addition of D_2O to the freeze-dried protein: 10, 20, and 30 (all 2 scans/ t_1 increment); 45, and 98 (4 scans/ t_1 increment); 340 (8 scans/ t_1 increment); 640, 1200, 1890, and 2460 min (16 scans/ t_1 increment). Because of the manner in which the experiments were recorded, the time points listed here represent the midpoints of the individual experiments as actually recorded. Amide NH exchange rates were measured by following the intensity of the ^{15}N - 1H correlation cross-peaks over the course of the experiments. Polynomial base-line corrections of order 3 were applied to the transformed spectra in each dimension. After the various processed spectra were scaled for the different number scans for each t_1 increment, cross-peak volumes were measured by using the Bruker UXNMR software running on a Bruker X32 computer. The decay of cross-peak intensity with time was found to be exponential within experimental error. These experimental decays were best fitted to a single exponential by using Powell's method of nonlinear least-squares optimization (Powell, 1965).

RESULTS AND DISCUSSION

Our analysis of the secondary structure of IL-1 β is based on a detailed survey of readily identifiable NMR parameters associated with the resonances of the polypeptide backbone. These include short-range sequential NOEs, medium- and long-range NOEs between NH and $C^\alpha H$, NH and NH, and $C^\alpha H$ and $C^\alpha H$ resonances, the values of the $^3J_{NH\alpha}$ coupling constants, which relate to the backbone ϕ torsion angle, and the amide NH exchange rates, which indicate the pattern of hydrogen bonding. We discuss the measurement of each one of these sets of parameters in turn.

NOE Analysis. The pattern of short-range sequential backbone NOEs in globular proteins can, in certain circumstances (Wüthrich, 1986), yield an indication of the nature of the polypeptide conformation. Thus, extended regions of strong $C^\alpha H(i)$ -NH($i+1$) NOEs indicate that the polypeptide adopts an extended conformation such as that found in a β -strand. On the other hand, an extended run of strong NH(i)-NH($i+1$) NOEs may indicate an α -helical structure. The

major element in the analysis of protein secondary structure from NMR data comprises the identification of medium- and long-range backbone-backbone NOEs. Thus α -helices are identified by the presence of medium-range $C^{\alpha}H(i)-NH(i+3,4)$ and $C^{\alpha}H(i)-C^{\beta}H(i+3)$ NOEs. Both parallel and antiparallel β -sheet structures are associated with long-range $NH(i)-C^{\alpha}H(j)$ and $NH(i)-NH(j)$ NOEs where residues i and j are usually more than five positions apart in the protein sequence. Antiparallel β -sheet structures are also characterized by $C^{\alpha}H(i)-C^{\alpha}H(j)$ NOEs.

The identification of short-range NOEs naturally falls out of the process of sequence-specific resonance assignment. Recently, we reported the complete sequence-specific assignment of the backbone resonances of IL-1 β (Driscoll et al., 1990). These assignments were obtained from an analysis of 3D $^{15}N-^1H$ heteronuclear NOESY-HMQC and HOHAHA-HMQC spectra of IL-1 β . To obtain the pattern of long-range NOEs involving amide NH protons requires a complete analysis of the 1H NOESY spectrum of the protein recorded in H_2O solution. Again, these 3D heteronuclear experiments provide the most useful means of performing the NOE analysis. The spectra obtained with these pulse sequences have the advantage that for IL-1 β cross-peak overlap is almost entirely removed from the spectrum, allowing an essentially complete analysis of the NOE connections. Thus the spectra are virtually devoid of any ambiguity caused by NH chemical shift degeneracy. It is worthwhile noting that the sensitivity of these experiments is so good that, in practice, all NOEs that are detectable in the regular 1H 2D NOESY spectrum are also detectable in the 3D NOESY-HMQC spectrum, including those that are very weak in intensity, as is often the case for long-range NOEs.

For a complete description of the theory and application of the 3D heteronuclear experiments to ^{15}N -labeled proteins, the reader is referred to previous articles (Kay et al., 1989a; Marion et al., 1989a,b; Driscoll et al., 1990; Fesik & Zuiderweg, 1988; Zuiderweg & Fesik, 1989). The concept behind the design of these 3D heteronuclear experiments is essentially very simple. Thus the experiments can be regarded as the combination of two 2D pulse sequences, in which the acquisition period of a regular 2D NOESY or HOHAHA experiment is replaced by the evolution, mixing, and detection periods of the HMQC experiment. The principles of the 3D NOESY and 3D HOHAHA experiments are essentially identical. Let us consider the 3D NOESY-HMQC pulse sequences. During the first half of the experiment, $^1H-^1H$ NOEs are generated involving the amide NH protons. The amide NH magnetization is modulated as a function of t_1 by the chemical shifts of those protons to which they are connected by NOEs. In the second half of the experiment, the magnetization of the amide protons is selected via the filtering effect of heteronuclear multiple-quantum-coherence (HMQC) pulse sequence. At the same time the amide proton magnetization is modulated as a function of t_2 by the directly bonded ^{15}N chemical shift. The resulting signal is measured as a function of t_3 . After Fourier transformation with respect to all three time variables t_1 , t_2 , and t_3 , a 3D spectrum is obtained with 1H axes F_1 (all protons) and F_3 (amide NHs only), and a ^{15}N axis F_2 . The most convenient way to visualize the resulting spectrum is as a regular 2D $\omega_2-^{15}N$ -edited NOESY spectrum (Fesik et al., 1987) with the F_2 1H axis relabeled F_3 . The spectrum has been "stretched out" in a direction perpendicular to the F_1-F_3 plane, along the ^{15}N axis labeled F_2 . Each F_1-F_3 plane of the 3D spectrum covers the same region as the regular 2D experiment, but contains many fewer

cross-peaks. Thus, resolution in the 3D experiment is improved relative to the 2D experiment because all peaks are spread over a 3D space, rather than a 2D plane. In favorable circumstances, such as was found in the case of IL-1 β , these experiments can lead to the essentially complete resolution of the amide NH region of the $^1H-^1H$ NOESY spectrum (Driscoll et al., 1990).

Short-Range NOEs. It was clear from our previous work on the sequence-specific assignment of the spectrum of IL-1 β that the major part of the polypeptide chain is in an extended conformation, as suggested by the predominance of strong $C^{\alpha}H(i)-NH(i+1)$ NOEs throughout the whole protein chain (Driscoll et al., 1990). In addition, there is a very high incidence of sizable $C^{\beta}H(i)-NH(i+1)$ NOEs, which further supports the conclusion that the protein contains a very high proportion of β -strand structures. No regions of α -helical structure can be identified from these data. All this is consistent with the general appearance of the NMR spectrum of IL-1 β , which shows good dispersion of the amide NH and $C^{\alpha}H$ resonances, as well as that of the circular dichroism spectrum of IL-1 β (Craig et al., 1987). Both of these indicate that IL-1 β contains a very high proportion of β -sheet structure with no α -helix content.

Long-Range NH- $C^{\alpha}H$ and NH-NH NOEs. Figure 1 shows a small section of the "reduced" 3D NOESY-HMQC spectrum of ^{15}N -labeled wild-type IL-1 β . The figure shows a composite of narrow strips of 2D contour plots that are taken from different slices of the 3D NOESY-HMQC spectrum. Each slice of the 3D spectrum, taken at a particular ^{15}N chemical shift, contains only those cross-peaks that arise from amide NH groups whose ^{15}N chemical shifts lie in a very narrow range. Each strip in Figure 1 contains those NOEs that connect a particular amide NH (F_3 dimension) with other NH, aromatic, and aliphatic protons (F_1 dimension). For a full description of this treatment of the data available from the heteronuclear 3D spectrum, the reader is referred to Driscoll et al. (1990). In Figure 1 the strips are arranged in sequence order according to the assignment of the amide NH in each strip. Thus, the figure shows those NOEs that correlate with the amide NHs of residues Ser-17-Leu-29. A blank strip is inserted for Pro-23, which does not possess an amide proton. An asterisk within each strip indicates the position of the intense diagonal peak, thus marking the chemical shift of the NH proton. A box labels the position of the intraresidue NH- $C^{\alpha}H$ cross-peak, as detected in the corresponding position in the 3D HOHAHA-HMQC spectrum. A number of long-range NOE connections are indicated by the arrows. These include NH-NH connections between residues Gly-22 and Glu-25, Val-19 and Lys-27, Ser-21 and Lys-27, and Ser-17 and Leu-29, together with the following NH- $C^{\alpha}H$ connections: Val-19 \rightarrow Ala-28, Leu-29 \rightarrow Leu-18, Lys-27 \rightarrow Leu-18, Lys-27 \rightarrow Met-20, Glu-25 \rightarrow Met-20, Val-19 \rightarrow Leu-26, Ser-21 \rightarrow Leu-26, Gly-22 \rightarrow Met-20, and Gly-22 \rightarrow Leu-26. These NOEs, together with long-range $C^{\alpha}H-C^{\alpha}H$ NOEs between residues Met-20 and Leu-26, and Ala-28 and Leu-18 (see below), clearly indicate a section of antiparallel β -sheet, connected by a short hairpin loop comprising residues Gly-22, Pro-23, and Tyr-24.

It has been possible to perform a virtually complete analysis of the amide region of the NOESY spectrum of IL-1 β by using the heteronuclear 3D spectra. Additional medium- and long-range NOE analysis was performed by using 2D spectra of the wild-type protein recorded at 27 $^{\circ}C$, as well as the 1H 2D H_2O NOESY, HOHAHA, and COSY spectra of des-[Ala-1], K27C, K93A, and K94A mutants of IL-1 β at 36 $^{\circ}C$.

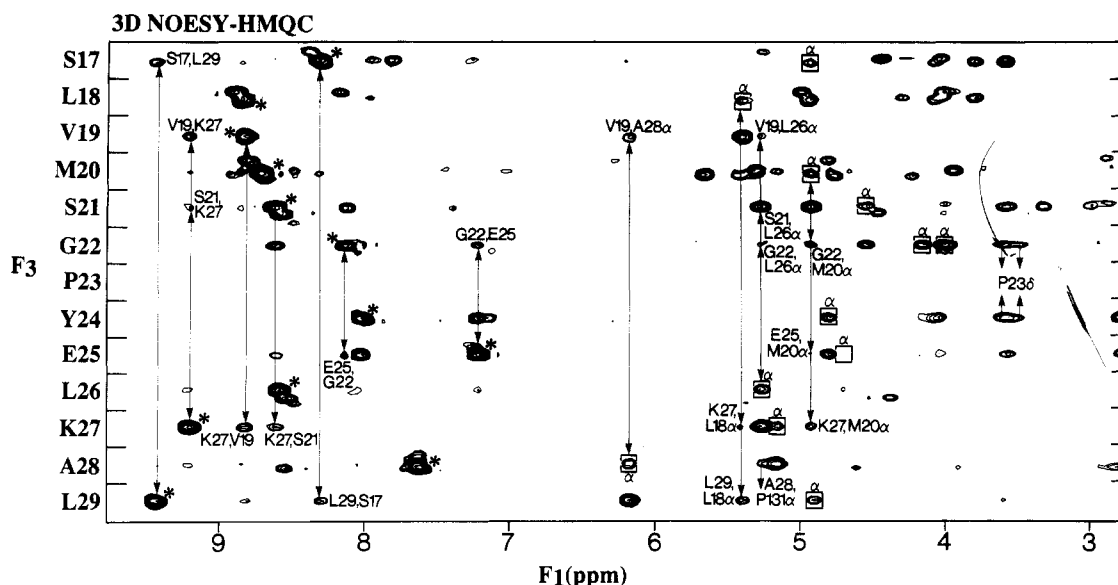


FIGURE 1: A small region of the "reduced" 3D ^{15}N - ^1H NOESY-HMQC spectrum of ^{15}N -labeled wild-type IL-1 β at pH 5.4 and 36 °C. This figure is composed of narrow strips taken from different F_1 - F_3 planes of the 3D spectrum [see Driscoll et al. (1990) for details]. The cross-peaks that fall on the center line of each strip originate from a single amide NH proton. The strips have been selected from the plane in which the NOEs of interest exhibit maximum intensity and have been placed in order of the primary sequence based on the previously reported amide NH assignments (Driscoll et al., 1990). An empty strip has been inserted for Pro-23, which has no NH proton. Tick marks on the left and right of the spectrum indicate the division of the strips. Asterisks mark the positions of the relatively intense "diagonal" peak, and a box indicates the position of the C^αH resonance for each residue based on the location of intrasidue $\text{NH}-\text{C}^\alpha\text{H}$ cross-peaks in the 3D ^{15}N - ^1H HOHAHA-HMQC spectrum (not shown). The good resolution of the 3D spectrum allows a relatively straightforward assignment of long-range NOEs. A number of long-range NH-NH and NH- C^αH NOEs are indicated.

Each of these different proteins retains the overall three-dimensional fold of the wild-type protein as judged from the general conservation of chemical shifts. The only significant chemical shift changes observed for these proteins could be attributed to residues either close to the site of mutation in the primary sequence of the protein or spatially proximate in terms of the secondary structure mapped out by this work. In the fingerprint region of the spectrum no chemical shift differences greater than 0.2 ppm could be detected. This result indicates that the side chains of the mutated lysine residues do not reside in the core of the protein but are located on the surface of the protein. However, the small chemical shift differences that are present between these proteins allow the resolution of some ambiguity that arises from chemical shift degeneracy in the spectra of the wild-type protein. We note in passing that the general strategy of replacing charged side chains with a residue such as alanine, which is readily detected in protein 2D spectra, allows an easy method of confirming sequence-specific assignments, as well as being extremely useful in the investigation of the structure-function relationship for the protein, where the protein surface is of most interest.

Long-Range C^αH NOEs. A second category of long-range NOEs that is useful in the identification of secondary structure elements, is derived from the aliphatic region of the NOESY spectrum recorded in D_2O solution. In particular, antiparallel β -sheet structure elements should give rise to strong long-range $\text{C}^\alpha\text{H}-\text{C}^\alpha\text{H}$ NOEs. The region of the 2D ^1H D_2O NOESY spectrum of IL-1 β containing these NOEs is shown in Figure 2. The mixing time used for this experiment was 100 ms. The large number of long-range $\text{C}^\alpha\text{H}-\text{C}^\alpha\text{H}$ NOEs present suggests that the β -strands of IL-1 β are predominantly arranged in anti-parallel β -sheets. These NOEs could be identified on the basis of the sequence specific assignments that we have previously reported (Driscoll et al., 1990).

$^3J_{\text{NH}\alpha}$ Coupling Constants. A further criterion for judging the nature of the conformation of the polypeptide backbone is the magnitude of the $^3J_{\text{NH}\alpha}$ coupling constants. The size

of $^3J_{\text{NH}\alpha}$ can be related, via a Karplus relationship, to the value of the ϕ dihedral angle (Karplus, 1963; Pardi et al., 1984). Thus, a small $^3J_{\text{NH}\alpha}$ coupling constant (<5 Hz) is indicative of a value of ϕ between -80 and -40° , such as is commonly found in α -helical structures. A large value of the $^3J_{\text{NH}\alpha}$ coupling constant (>8 Hz) suggests a ϕ value in the range -150 to -90° , consistent with an extended backbone conformation, as is the case, for example, in a β -strand. Obtaining accurate estimates of the $^3J_{\text{NH}\alpha}$ coupling constants in large proteins by the traditional measurement of antiphase multiplet splittings of fingerprint region cross-peaks in ^1H correlated spectra is rendered extremely difficult because of the large amide NH proton line widths. Recently, methods have been designed to measure $^3J_{\text{NH}\alpha}$ coupling constants in proteins labeled with ^{15}N based on the heteronuclear multiple-quantum-coherence experiment (Kay & Bax, 1990). These experiments take advantage of the longer ^{15}N - ^1H multiple-quantum transverse relaxation times, and hence narrower line widths, and the $\text{NH}-\text{C}^\alpha\text{H}$ homonuclear J coupling modulation of the ^{15}N magnetization during F_1 to measure the J splittings. The particular method we adopted utilizes a variant of the HMQC-COSY experiment (Gronenborn et al., 1989a), known as HMQC- J , in which estimates of the $^3J_{\text{NH}\alpha}$ coupling constants are obtained from the splittings detected in the F_1 cross sections of the ^{15}N - ^1H correlation cross-peaks. These estimates of the $^3J_{\text{NH}\alpha}$ coupling constants are then corrected for the effects of a finite line width and the presence of a small dispersive contribution to the line shape. This is achieved by best fitting the measured splittings obtained by using three different apodization functions in the processing of the F_1 dimension, with theoretically calculated line shapes (Kay & Bax, 1990; Forman-Kay et al., 1990).

As described previously, samples of IL-1 β purified from the wild-type gene construct are in fact an approximate 3:2 mixture of wild-type unprocessed IL-1 β and a processed form of the protein in which the N-terminal alanine has been cleaved, denoted as des-[Ala-1] IL-1 β (Driscoll et al., 1990).

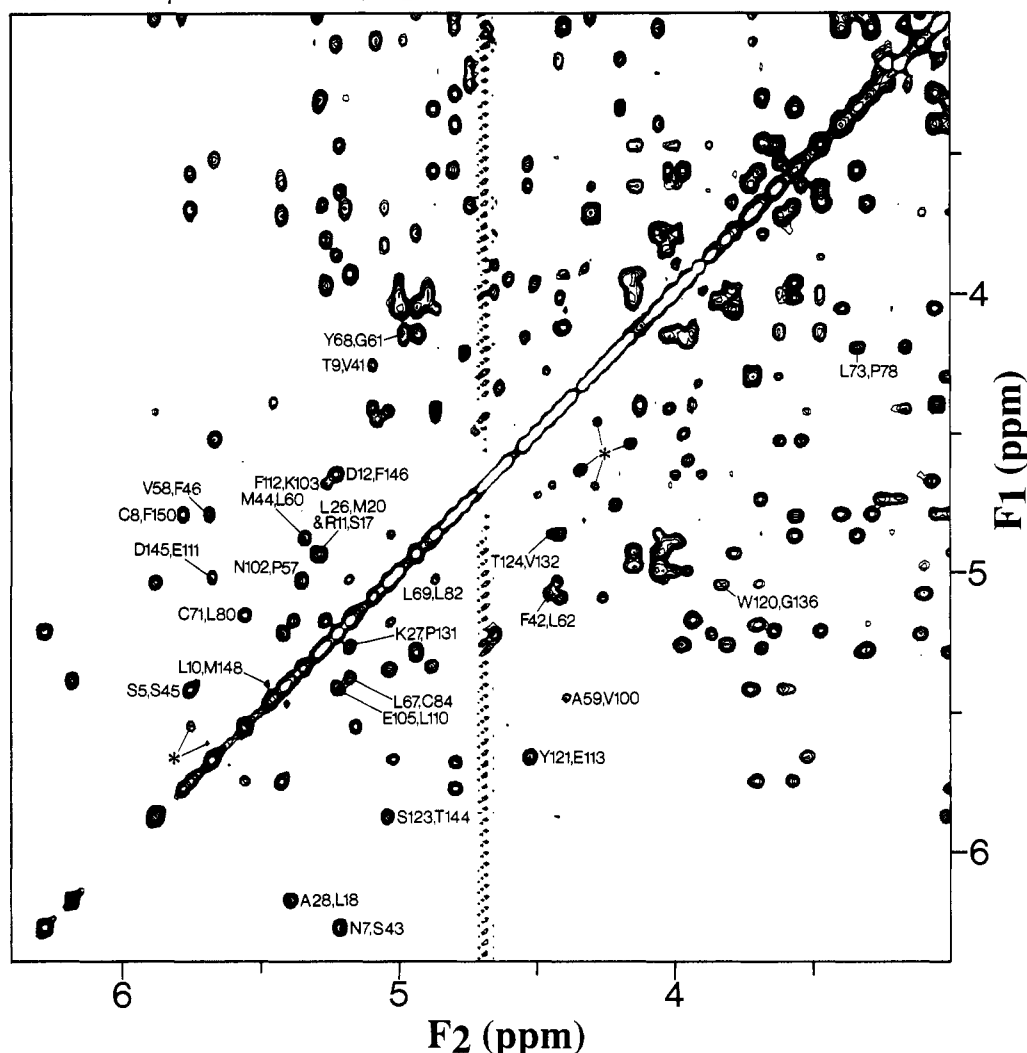
Interleukin-1 β : 100 ms NOESY D₂O

FIGURE 2: C α H region of the 2D 1 H 100-ms D₂O NOESY spectrum of wild-type IL-1 β , pH 5.4 and 36 $^{\circ}$ C. A number of long-range C α H-C α H NOEs are indicated. Asterisks indicate cross-peaks that have been attributed to a slow conformational exchange processes (see text).

As we have shown in our previous paper, the spectral differences between unprocessed IL-1 β and des-[Ala-1] IL-1 β are small, leading to resolvable differences in chemical shifts for the amide NH 15 N and 1 H resonances of only a small number of residues. However, application of the HMQC-*J* experiment to this mixture of two protein forms yielded uninterpretable results for a large number of cross-peaks. This difficulty is attributed to the presence of small unresolved chemical shift differences for the two protein species, which are otherwise not detected within the line width of the cross-peak. Coupling constants were therefore measured on the chemically homogeneous des-[Ala-1] IL-1 β sample, thereby circumventing the above complications. Because of the good resolution of the 15 N- 1 H correlation peaks in the HMQC-*J* experiment it was possible to measure 97 $^3J_{\text{NH}\alpha}$ coupling constants from a single experiment. These values are plotted as a function of amino acid sequence in Figure 3A. As there is no evidence from the analysis of NOE data that the three-dimensional structures of the unprocessed wild-type and des-[Ala-1] proteins are different within experimental error, we believe it is justified to use coupling constant measurements from the des-[Ala-1] form of the protein in the context of the structure of the unprocessed wild type.

The smallest measured $^3J_{\text{NH}\alpha}$ coupling constant was 5.3 Hz, which is considerably smaller than could possibly be measured from a regular H₂O COSY spectrum of this protein. The

largest measured $^3J_{\text{NH}\alpha}$ coupling constant was 9.9 Hz. The majority of coupling constants fell in the range of 8.0–10.0 Hz, consistent with values of ϕ indicative of extended β -strand polypeptide chains. A number of peaks did not exhibit a measurable splitting. These cross-peaks could be divided into three classes: peaks that clearly exhibited good signal to noise ratio and therefore were assumed to possess relatively narrow 15 N and 1 H line widths; peaks that had a poor signal to noise ratio and appeared to possess relatively broad 15 N or 1 H line widths; and peaks that could not be interpreted because of cross-peak overlap. Cross-peaks in the first category (of which there are 14) were assigned $^3J_{\text{NH}\alpha}$ coupling constant values of <5.0 Hz. No values for the coupling constant were assumed for the other two categories.

Amide NH Exchange Rates. The identification of slowly exchanging protons can be used to help identify hydrogen-bonded groups within the protein. In combination with certain recognizable patterns of short-, medium-, and long-range NOEs, the presence of slowly exchanging amide NH resonances can be rationalized in terms of regular secondary structure elements (Wüthrich et al., 1984; Wüthrich, 1986). We have made accurate measurements of the exchange rates of 73 slowly exchanging amide NH groups in IL-1 β by following the intensities of the 15 N- 1 H correlation peaks in a series of double INEPT "Overbodenhausen" experiments recorded after dissolving freeze-dried protein into D₂O. Figure

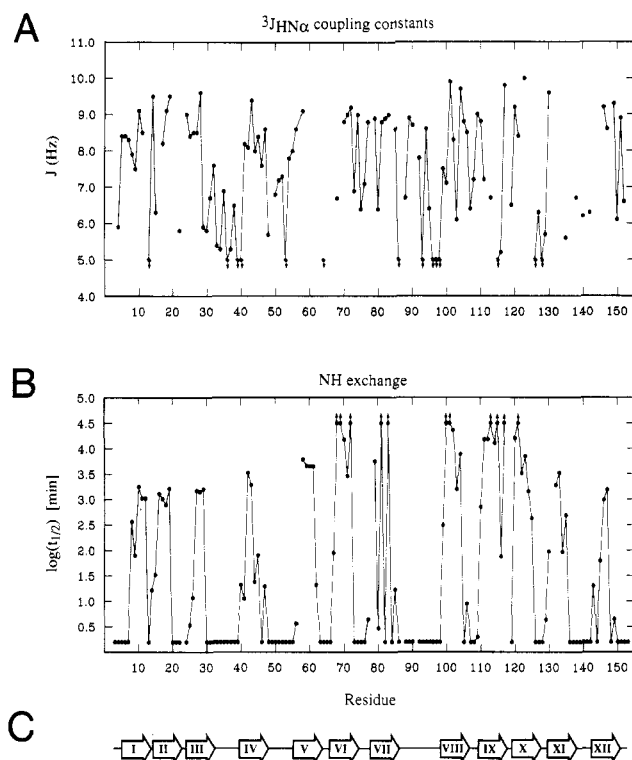


FIGURE 3: (A) $^3J_{NH\alpha}$ coupling constants obtained for ^{15}N -labeled des-[Ala-1] IL-1 β plotted as a function of residue number. The values for $^3J_{NH\alpha}$ were obtained by using the HMQC- J pulse sequence and have been corrected for the contributions due to dispersive and finite line-width contributions to the line shape. Residues exhibiting a small ^{15}N - 1H multiple-quantum line width but no measurable splitting have been assigned a $^3J_{NH\alpha}$ value of <5.0 Hz, as indicated by the downward pointing arrows. (B) Amide NH/solvent exchange half-lives plotted as a function of residue number. These measurements are based on the observed time dependence of the intensity of the ^{15}N - 1H cross-peaks in an inverse "Overbodenhausen" correlation experiment, after dissolving freeze-dried ^{15}N -labeled wild-type IL-1 β in D_2O solution at $36^\circ C$, pH 6.1. Residues with amide NH/solvent exchange half-lives shorter than 3 min or longer than 3×10^4 min could not be estimated from the experimental data. The former are arbitrarily plotted with $\log t_{1/2} = 0.2$; the latter are indicated by the upward pointing arrows. (C) Schematic representation of the polypeptide chain of IL-1 β showing the approximate locations of the 12 β -strands within the protein sequence as identified from the NMR parameters described in the text.

4 shows 4 of a series of 10 of these heteronuclear correlation spectra recorded as a function of time after the addition of D_2O to the protein. The first spectrum was recorded within 10 min, starting 5 min after the addition of D_2O to the protein. Four experiments were recorded within the first hour of exchange, resulting in reasonable time resolution for the measurement of the exchange rates for those amides that are fully exchanged within that time period. The Overbodenhausen experiment applied to a ^{15}N -labeled protein sample can be recorded in much shorter time than a 1H 2D COSY, HOHAHA, or NOESY experiment and can therefore yield extremely good time resolution for the measurement of NH exchange rates. After all 10 spectra were suitably scaled, the cross-peak intensities were quantified by measurement of the cross-peak volumes, and the exchange rates were calculated by best fitting the time dependence to a single-exponential decay. The experimentally determined half-lives of the slowly exchanging amide protons are plotted as a function of protein sequence in Figure 3B. Amide protons that were not detectable in the first spectrum recorded in the series (midpoint 10 min after addition of D_2O to the freeze-dried IL-1 β sample, Figure 4A) were thus assigned a half-life of <2 min. Amide

NHs with half-lives significantly longer than 10 min can reasonably be assumed to be involved in hydrogen bonding in the interior of the protein. An alternative explanation for slow exchange behavior is that the proton is solely buried in a solvent-inaccessible region of the protein. Consequently, specific hydrogen bonds can only be invoked in the presence of a supporting pattern of NOEs. Thus, in the case of an antiparallel β -sheet, a hydrogen bond can be assigned between the NH of residue i on one β -strand to the carbonyl group of residue j on the opposite antiparallel β -strand in the presence of the following NOEs: $NH(i)-NH(j)$, $NH(i)-C^{\alpha}H(j+1)$, $C^{\alpha}H(i-1)-C^{\alpha}H(j+1)$. Additionally, in a regular antiparallel β -sheet the $NH(i)-CO(j)$ hydrogen bond will be accompanied by a $NH(j)-CO(i)$ hydrogen bond and the corresponding $NH(j)-C^{\alpha}H(i+1)$ and $C^{\alpha}H(j-1)-C^{\alpha}H(i+1)$ NOEs.

Secondary Structure Analysis. A complete analysis of the NMR parameters pertinent to the determination of secondary structure elements has been performed. The results of this analysis are summarized in Figure 5, which shows a scheme of the regular secondary structure of the polypeptide chain of IL-1 β . The medium- and long-range NOEs, and hydrogen bonds that have been assigned on the basis of the amide NH exchange rate measurements, are indicated. The structure that has been identified consists of a series of 12 antiparallel β -strands that extends over almost the entire length of the protein sequence. The 12 strands, indicated by roman numerals, run between the following residue numbers: strand I, Ser-5–Ser-13; strand II, Gln-15–Ser-21; strand III, Glu-25–Leu-31; strand IV, Val-41–Val-47; strand V, Ile-56–Lys-63; strand VI, Asn-66–Val-72; strand VII, Pro-78–Val-85; strand VIII, Val-100–Ile-106; strand IX, Lys-109–Ala-115; strand X, Trp-120–Ser-125; strand XI, Met-130–Gly-136; and strand XII, Asp-145–Phe-150. The presence of 12 strands in the complete secondary structure analysis is consistent with the recognizable groupings of residues exhibiting strong $C^{\alpha}H(i)-NH(i+1)$ and $C^{\beta}H(i)-NH(i+1)$ short-range sequential NOEs. The approximate positions of these 12 strands are indicated by the numbered arrows along the protein sequence ordinate in Figure 3C. Careful inspection of Figure 3 shows that the positions of the 12 β -strands show a very good correlation with the presence of relatively large values of the $^3J_{NH\alpha}$ coupling constant (>8.0 Hz) and slowly exchanging amide NH protons. In the same manner, the regions of protein sequence lying between the individual β -strands exhibit a higher population of small $^3J_{NH\alpha}$ coupling constants (<7.0 Hz) and amide NHs that exchange more rapidly in D_2O .

The 12 strands can be connected into a single extended network of antiparallel β -sheets. For the purposes of illustrating the structure, the extended β -sheet network has been broken up into two halves (Figure 5). Figure 5A shows a section that contains a skewed six-stranded antiparallel β -sheet structure comprising strands XII, I, IV, V, VIII, and IX. There appears to be a hairpin turn connecting strands VIII and IX. On the basis of the strong $NH(i)-NH(i+1)$ NOEs between residues Asn-107 and Asn-108 and residues Asn-108 and Lys-109, the turn can be assigned to the type I variety (Richardson, 1981). A longer loop must be invoked to connect strands IV and V. Note that the antiparallel arrangement of strands IX and XII appears at both the top and bottom of this sheet as shown in Figure 5A. This arrangement indicates that the six-stranded antiparallel β -sheet is twisted into a β -barrel structure. Attached to this six-stranded β -sheet structure are β -turns between strands I, V, and IX and the N-terminal portions of strands II, VI, and X, respectively. The presence of strong $NH(i)-NH(i+1)$ NOEs between residues Asn-66

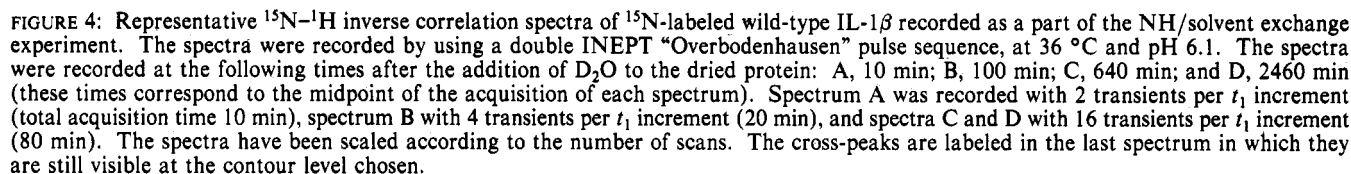


Figure 5B shows two extra sections of secondary structure obtained from the analysis of NMR parameters. Both of these sections are contiguous with the section of secondary structure shown in Figure 5A. The first extra portion of secondary structure comprises a pair of regular antiparallel β -sheets (strands X and XI, and II and III) loosely connected in an antiparallel fashion at the interface of strands III and XI. A loop of unidentified structure connects strands X and XI between residues Ser-125 and Asn-129. None of the residues Gln-126, Ala-127, and Glu-128 exhibits a NH/solvent ex-

The remaining parts of the polypeptide chain that have not been accounted for in the β -sheet network shown in Figure 5 include the N- and C-terminal regions and long loops that must be invoked to join strands III and IV between Leu-31 and Val-41, strands VII and VIII between Val-85 and Val-100, and strands XI and XII between Gly-136 and Asp-145. The C- and N-terminal portions of the polypeptide chain come together in the antiparallel pairing of strands I and XII (Figure 5A). No regular structure can be detected for the first four residues of the protein's N terminus, Ala-1-Arg-4, or the last three residues of the C terminus, Val-151-Ser-153. This result is interesting in the light of biological studies that have focused on the C- and N-terminal parts of the IL-1 β molecule. We have previously reported that N-terminal methionylated IL-1 β has a 10-fold reduced receptor binding affinity compared to the wild-type protein (Wingfield et al., 1987c). In addition, an IL-1 β construct containing an additional cysteine residue at the N terminus (Ala-Cys-Pro...) modified at the cysteine with streptavidin was unable to bind to the IL-1 receptor,

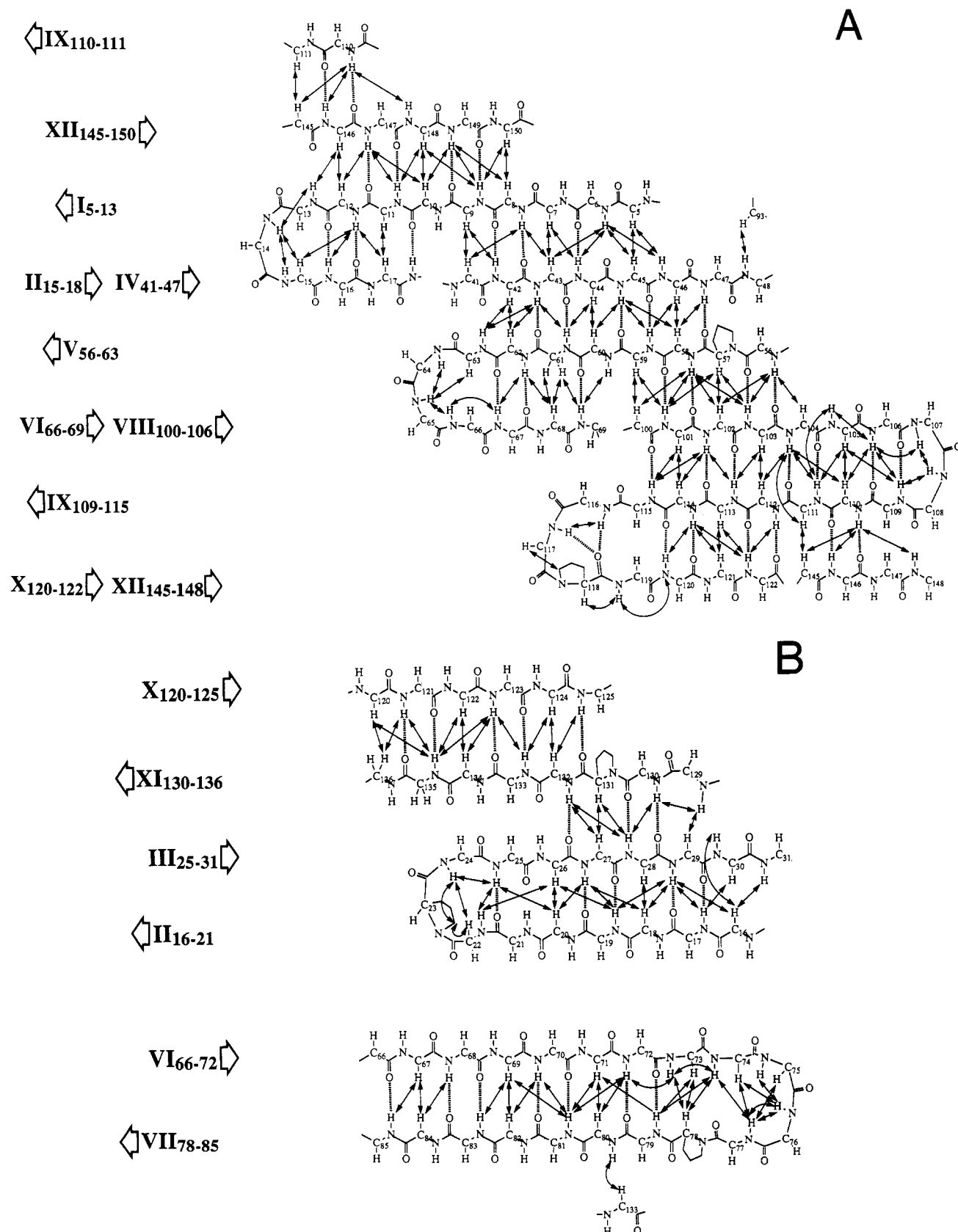


FIGURE 5: Secondary structure elements of IL-1 β as determined from the analysis of NMR parameters described in this paper. The β -strands are indicated on the left by roman numerals and the residue number range. Long-range NOEs are indicated by the arrows, and hydrogen bonds derived from the NH/solvent exchange and NOE data are illustrated by broken lines. Part A contains the six-stranded antiparallel β -sheet that is folded into a β -barrel.

whereas modification at the cysteine with small molecular weight modifiers had no significant effect on receptor binding (P.T.W., unpublished data). These results suggest that modification of the N terminus of IL-1 β can cause a pertur-

bation of the receptor-binding region of the protein. On the other hand, it has been observed that the functional integrity of the molecule is essentially completely retained when either of the N-terminal sequence Ala-1-Pro-2-Val-3 or of the C-

Table I: Location of β -Strands in IL-1 β Determined by NMR and X-ray Diffraction

strand	residue range		strand	residue range	
	NMR ^a	X-ray ^b		NMR ^a	X-ray ^b
I	Ser-5– Ser-13	Val-3– Asp-12	VII	Pro-78– Val-85	Lys-77– Pro-87
II	Gln-15– Ser-21	Gln-15– Gly-22	VIII	Val-100– Ile-106	Lys-97– Ile-104
III	Glu-25– Leu-31	Glu-25– Gly-33	IX	Lys-109– Ala-115	Asn-107– Glu-113
IV	Val-41– Val-47	Gln-38– Gln-48	X	Trp-120– Ser-125	Pro-118– Thr-124
V	Ile-56– Lys-63	Asp-54– Leu-62	XI	Met-130– Gly-136	Met-130– Gly-136
VI	Asn-66– Val-72	Lys-65– Lys-74	XII	Asp-145– Val-150	Asp-142– Ser-152

^a This work. ^b From Table I of Priestle et al. (1988).

terminal sequence Val-151-Ser-152-Ser-153 is missing (Mosley et al., 1987). Further removal of residues from the C terminus, including Phe-150, Gln-149, Met-148, and Thr-147, which are in a β -sheet according to our work, sequentially reduced the biological activity of the protein to less than detectable levels (Mosley et al., 1987). It has been suggested that residues near the N terminus are implicated in the receptor binding of IL-1 β . In particular, the exchange of Arg-4 for a glutamic acid residue in a IL-1 β protein containing other N-terminal mutations reduces receptor binding affinity by a factor of 200 (Huang et al., 1987). In contrast to this report, we have found that the des-[Ala-1] mutant and an N-terminal cleavage product that has lost the first four amino acids exhibit comparable binding affinities to wild-type IL-1 β (MacDonald, H. R. and Wingfield, P. T., unpublished results). In the present study, residues Ala-1–Arg-4 are not implicated in any regular secondary structure element but are attached to the start of the antiparallel β -sheet between strands I and XII. Thus, removal of the first four residues should not lead to any noticeable disruption of the stable secondary structure elements. We therefore believe that although N-terminal modifications may influence receptor binding, it is not the N terminus itself that is the direct site of interaction between the receptor and IL-1 β .

Comparison with the X-ray Crystal Structure of IL-1 β . Recently, an unrefined model (*R* factor of 42%) of IL-1 β was reported in the literature based on a crystallographic study at a resolution of 3 Å (Priestle et al., 1988). The limited structural details reported, the moderate resolution, and the lack of atomic coordinates meant that the X-ray model was of little use in the analysis of the secondary structure based on NMR parameters. Thus the analysis of the NMR data proceeded independently of the X-ray structure.

The X-ray data show the presence of 12 extended β -strands folded into a globular structure. More precisely, the crystal structure is described as consisting of six β -strands forming a β -barrel structure, which is closed off at one end by another six β -strands, adopting an exclusively antiparallel β -structure. While the current NMR data are insufficient to determine the precise nature of the fold of IL-1 β , it is instructive to compare the model three-dimensional structure obtained by X-ray diffraction with the secondary structure elements that have been identified in the current NMR investigation.

First, both studies have located 12 β -strands in the structure. Moreover, there is generally a good correspondence between the residue numbers locating each strand in the protein sequence. Table I lists the approximate locations of the 12 β -strands as found in the X-ray and NMR investigations. In some cases the β -strands identified in the X-ray study are defined as being slightly longer than those determined unam-

biguously from the NMR data. This may solely reflect the confidence level of the present NMR structure. Another pleasing correspondence between the two studies is the general agreement in the disposition of the individual strands in an antiparallel network. In particular, the NMR data clearly reveal the existence of a skewed six-stranded antiparallel β -sheet in which strand XII is hydrogen bonded to strand I, strand I to IV, strand IV to V, strand V to VIII, strand VIII to IX, and finally strand IX back to XII (Figure 5A), thus providing unambiguous evidence that these six strands form a β -barrel, in complete agreement with the X-ray analysis. The location of the tight turns/short loops versus the long loops is also in close agreement. Thus, in both the X-ray structure and the NMR secondary structure analysis, long loops are found to connect strands III to IV, VII to VIII, and XI to XII, whereas all other interstrand connections are made of shorter segments of polypeptide chain. One clear discrepancy, however, is apparent between the X-ray crystallography report of the IL-1 β structure and the present NMR work. In the assignment of the different β -strands in the crystal structure, strand VIII was assigned to residues Lys-97–Ile-104, and strand IX to residues Asn-107–Glu-113. Thus, the turn connecting strands VIII and IX in the crystal structure has been assigned to the residues preceding Asn-107. In contrast, the corresponding turn identified in the NMR structure comprises residues Ile-106–Asn-107–Asn-108–Lys-109 (see Figure 5A), with Asn-107 in position 2 of the turn. Since the criteria by which the β -strands were identified in the crystallographic model are not reported in the X-ray study, it is impossible at this stage to resolve this apparent disagreement. Suffice it to say that the location of this turn is unambiguously defined by the NOE data.²

Molecular Topology. The X-ray crystal structure of IL-1 β possesses a 3-fold internal structural pseudosymmetry, thought perhaps to arise from gene triplication followed by gene fusion (Priestle et al., 1988). A basis of this 3-fold symmetry can be detected in the current study of the secondary structure of IL-1 β by NMR. Careful consideration of the topology of strands involved in the formation of the extended β -structure shown in Figure 5 enables one to recognize a 3-fold repeated topology consisting of five β -strands. This topology is illustrated schematically in Figure 6a. The topological "unit" comprises five sequential β -strands of the protein, indicated by the letters A–E. Strands A and B and C and D, the C-terminal portion of strand B, and the N-terminal portion of strand C form β -hairpin structures. The C-terminal portion of strand E and the N-terminal portion of strand B also form an antiparallel β -sheet structure. Tight turns or short loops are found connecting strands A and B, B and C, and C and D. Strands D and E are connected by a longer stretch of polypeptide chain. This is the unit that can be detected experimentally on the basis of the NOE and slowly exchanging amide NH analysis presented above. The 3-fold repeat of this topology occurs with strands A–E equated with strands IV–VIII, VIII–XII, and XII plus I–IV. In the last case, the short loop between strands A and B is not formed but corresponds to the junction of the N- and C-terminal strands of the molecule in an antiparallel β -sheet arrangement. These experimental topologies are diagrammed schematically for the 12 β -strands of IL-1 β in Figure 6b–d. It is reported in the X-ray study that, in terms of the topology shown in Figure 6a, there is also antiparallel β -sheet formation between the C-terminal portion of strand C and the N-terminal portion of strand E (Priestle et al., 1988). This is indicated by the dotted extension of strand E in Figure 6a. In the current NMR study, however, we have

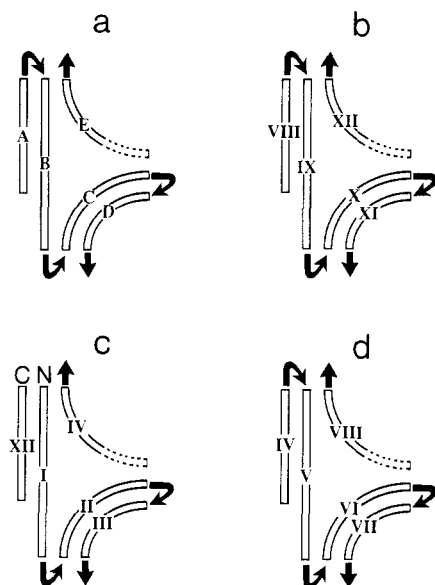


FIGURE 6: (a) The folding topology of β -strands that is found in the secondary structure of IL-1 β by NMR. This topology, which comprises five β -strands A-E, is repeated three times in the structure illustrated schematically in b-d. Curved arrows indicate tight turns or short loops. A long loop connects the C-terminal end of strand D with the N-terminal end of strand E. The dotted part of strand E illustrates the antiparallel β -sheet arrangement of the N-terminal segment of strand E and the C-terminal segment of strand C that has been observed in the unrefined model of IL-1 β obtained by X-ray crystallography (Priestle et al., 1988). This type of structure is not clearly detected in our NMR data.

found very limited evidence for such a structure. The only NOE evidence we have found is a long-range NOE between the C α H protons of Ser-123 and Thr-144. This brings strands X and XII into close proximity (Figure 6b). The secondary structure elements shown in Figure 5 account for the vast majority of amide NH groups with a solvent exchange half-life greater than 3 min. Of the remaining slowly exchanging NH groups, those of residues Val-40, Val-41, Cys-71, Phe-99, Val-100, Thr-124, Ile-143, and Asp-145 would potentially form antiparallel β -sheet between strands C and E of the topological unit (Figure 6a). However, the assignment of these parts of the polypeptide chain to regular secondary structure is not justified by the current level of NMR data and will have to await the determination of the full three-dimensional structure of IL-1 β in solution.

It is noteworthy that residues Leu-10 and Leu-60 are among those residues with the most slowly exchanging amide protons. Both are located at junctions between two portions of antiparallel β -sheet (see Figure 5A) and are most likely involved in hydrogen bonding. With respect to the topology of Figure 6a, these residues are located in the center of strand B with the amide NH presumably interacting with residues on strands C and E. At this stage of the investigation, however, no firm assignment to specific hydrogen bonds is possible.

In the X-ray model of IL-1 β , strands III, VII, and XI form a base of the six-stranded β -barrel (Priestle et al., 1988). In our NMR study, we detect several NOE and hydrogen bond interactions indicating an antiparallel arrangement of strands III and XI, as in the crystal structure (Figure 5B). Good evidence of antiparallel β -sheet formation between strands VII and XI, and III and VII, such as is reported for the X-ray model, is not found in the NMR data. Thus, the NOE evidence amounts only to a long-range NOE between the amide NH of Leu-80 and the C α H proton of Phe-133. However, the slow solvent exchange of the amide NH groups of Leu-80 and Leu-134 may indicate some as yet unidentified secondary

structure in this region of the protein.

Conformational Heterogeneity in the Structure of IL-1 β . During the course of the analysis of the 3D heteronuclear NOESY-HMQC and 2D 1 H NOESY spectra of IL-1 β it became clear that there were a number of cross-peak, resembling long-range NH-NH NOE connections, which were not consistent with the secondary structure results as presented in the sections above. On careful inspection of the corresponding 3D heteronuclear HOHAHA-HMQC and 2D 1 H HOHAHA spectra, these cross-peaks could also be found in the region containing only amide NH resonances. Ordinarily, HOHAHA spectra of globular proteins are devoid of cross-peaks in this region of the spectrum. These peaks possess the same sign as the diagonal peaks and are therefore not due to rotating frame NOE effects. The presence of these peaks in both the NOESY and HOHAHA spectra can be rationalized on the basis of one or a number of chemical exchange processes. In the simplest case, a two-site chemical exchange process occurring at a rate that is slower than $2\pi\Delta$, where Δ is the difference in chemical shift of the resonances for the two forms, may manifest itself as a single cross-peak symmetrically positioned on each side of the diagonal in both a NOESY or spin-lock (or HOHAHA) experiment, with sign equal to that of the diagonal signals (Jeener, 1979; Ernst et al., 1987).

Figure 7A shows a portion of the amide NH-amide NH region of an 80-ms 2D spin-lock experiment of wild-type IL-1 β recorded in H $_2$ O solution. In this experiment the transmitter offset was set to the left-hand edge of the spectrum and the spin-lock field was generated by a WALTZ-17 mixing sequence with the 17th pulse set to 180°. A weak spin-lock field of 5.5 kHz was used. The figure clearly shows a large number of NH-NH cross-peaks, indicating that a significant portion of the backbone is undergoing conformational exchange. These cross-peaks serve to complicate significantly the corresponding region of the H $_2$ O NOESY spectrum. Figure 7B shows the amide NH-amide NH region of a 100-ms 2D NOESY spectrum of wild-type IL-1 β , recorded under the same conditions as the spin-lock experiment of Figure 7A. The assignments of a number of these exchange cross-peaks are indicated. Note how the presence of these exchange cross-peaks, which in many cases are as intense as the authentic long-range NH-NH NOEs, severely complicates the analysis of this region of the NOESY spectrum.

It is worthwhile noting that these conformational exchange cross-peaks can be detected for both the authentic wild-type protein and the des-[Ala-1] form of IL-1 β , as is illustrated by the presence of a chemical exchange cross-peak for each of the resolved Arg-4 resonances (see Figure 7). Likewise the same sorts of exchange cross-peaks have been detected in the spectra of a number of point mutant IL-1 β proteins, including K27C-, K93A-, and K94A-IL-1 β . In addition, a number of similar exchange cross-peaks are visible in the C α H-C α H region of the D $_2$ O 2D 1 H NOESY and HOHAHA spectra of wild-type and K27C IL-1 β . The latter have been attributed to the conformational exchange phenomenon by elimination after the assignment of all scalar-coupled resonances in this region of the HOHAHA spectrum. Four prominent examples of these sorts of peaks are indicated by an asterisk in Figure 2. The unambiguous assignment of these peaks is awaiting the application of heteronuclear 13 C- 1 H 3D spectroscopy to uniformly 13 C labeled IL-1 β . Another interesting point is that the presence of the exchange cross-peaks appears to be insensitive to the experimental conditions. Thus, they are detected with approximately equal intensity in the pH interval

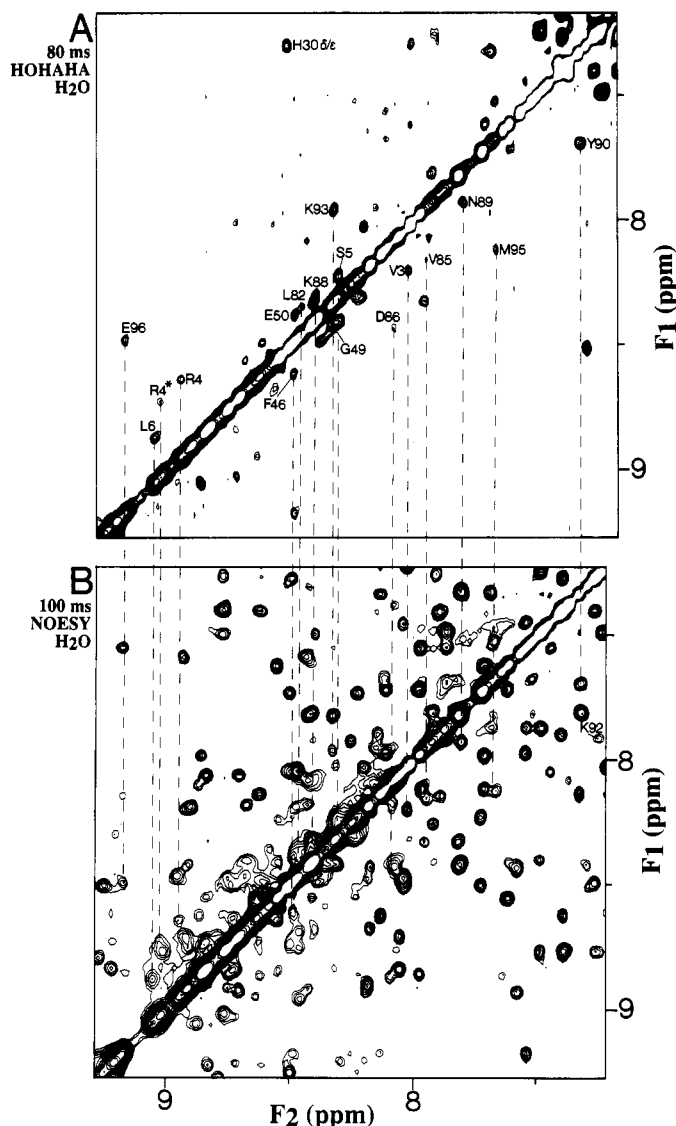


FIGURE 7: A portion of the amide NH–amide NH region of the spectrum of wild-type IL-1 β taken from (A) an 80-ms spin-lock experiment recorded with a WALTZ-17 mixing sequence and (B) a 100-ms NOESY spectrum recorded in H₂O at pH 5.4 and 36 °C. A number of peaks are observed close to the diagonal in the HOHAHA spectrum, which are attributed to a slow two-site conformational exchange process(es) in the protein. These “exchange” peaks also appear in the NOESY spectrum as shown by the dashed lines. The presence of these peaks complicates the long-range NOE analysis. Assignments for a number of these exchange peaks are shown. The chemical shift of the major form in the two-site exchange corresponds to the F_2 ordinate of the labeled cross-peak, the chemical shift of the minor form to the F_1 ordinate. The exchange peak due to Lys-92 is not clear in the HOHAHA spectrum, but is labeled in the NOESY spectrum. The strong scalar-coupled aromatic C^{δ1}H–C^{ε2}H cross-peak of His-30 is also labeled.

from 5.4 to 7.5, and for temperatures ranging from 20 to 40 °C.

While it has been possible to identify these rather unusual cross-peaks with at least one (and possibly several) conformational exchange process(es), it has proved impossible thus far to ascertain the precise source(s) of the phenomenon. The nature of the problem is illustrated in Figure 8, which shows small regions of the 100-ms NOESY and 30-ms HOHAHA 2D spectra of wild-type IL-1 β . The cross-peaks of the most downfield shifted amide NH resonances are highlighted (a prime denotes the peak due to the minor form). In this region of the 2D spectrum, the two sets of peaks for residue Gln-81 are just resolved from the rest of the spectrum. Gln-81 is one

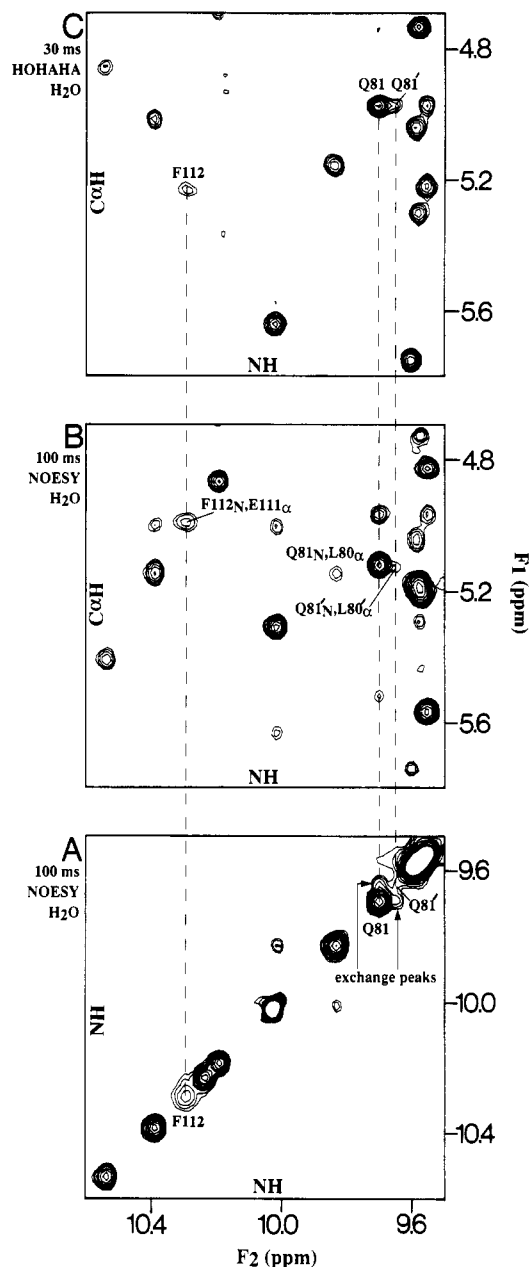


FIGURE 8: (A) A small region of the 100-ms H₂O 2D NOESY spectrum of wild-type IL-1 β recorded at 36 °C and pH 5.4. The exchange cross-peaks attributed to the conformational exchange are indicated for residue Gln-81. The peaks due to the minor form of the protein are denoted by primes. Also labeled is the diagonal cross-peak of Phe-112. Note the broad shape of the NH resonance for this residue compared to the other resolved amide diagonal peaks (the very intense peak in the center of the figure is an overlap of the amide NH of Val-58 and the ring N^H resonance of Trp-120). (B) A second region of the NOESY spectrum highlighting the NH($i+1$)–C α H(i) cross-peaks of Gln-81, Gln-81', and Phe-112. (C) The region of the 30-ms HOHAHA spectrum corresponding to (B), recorded under identical conditions. The intrasidue NH–C α H cross-peaks of Gln-81, Gln-81', and Phe-112 are labeled.

of those residues that exhibits chemical exchange cross-peaks as is illustrated in Figure 8A, which shows the amide NH–amide NH region of the 100-ms H₂O NOESY spectrum. In this case, where the peaks of the two exchanging resonances can clearly be resolved on the spectrum diagonal, it is possible to see that the populations of the two forms are very different. Indeed, as judged by the relative heights of the diagonal peaks for the two forms, we can estimate that the population of the minor form is of the order of <20% of the total protein concentration. This is borne out by the very weak intensity of

the interresidue Gln-81'→Leu-80' NH(*i* + 1)–C^αH(*i*) NOE in Figure 8B and the Gln-81' intraresidue NH(*i*)–C^αH(*i*) cross-peak in the HOHAHA spectrum shown in Figure 8C. Despite the different populations of the two forms of the protein, the exchange cross-peaks themselves are of a greater intensity than the diagonal peak of the minor form. Simulation of the equations that describe the time dependence of the amplitudes of the cross and diagonal peaks in the case of a two-site chemical exchange system with unequal populations (McConnell, 1958) shows that the exchange cross-peak can never exceed the amplitude of the diagonal peak of the minor form in a spectrum recorded with zero mixing time. In the limit of long mixing times the ratio of the intensities of the diagonal peak of the major form to the exchange cross-peak gives the equilibrium constant.

Based on the chemical shift differences for the two amide NH peaks of Gln-81 (0.05 ppm), an upper estimate of the exchange rate (given by the sum of the forward and backward rates) for the Gln-81 ↔ Gln-81' transition can be taken as ~200 s⁻¹. Additionally, for exchange cross-peaks to be observed in the NOESY spectrum, the rate constant for the slow transition should be greater than ~1/(20*T*₁) and the overall exchange rate (given by the sum of the forward and backward rates) should be greater than ~1/(5*T*₁), where *T*₁ is the longitudinal relaxation time of the NH protons. The *T*₁'s for the NH protons of IL-1β are about 0.7–0.8 s, so a lower limit for the rate constant for the slow Gln-81→Gln-81' transition is approximately 0.06 s⁻¹, while that for the overall exchange rate is ~0.25 s⁻¹. Further quantitative studies of this conformational equilibrium are in progress, along with a detailed investigation of the backbone dynamics based on ¹⁵N relaxation and heteronuclear NOE data (Kay et al., 1989c).

Because the minor form of the protein is present in a small amount compared to the major form, it has not proved possible to characterize its conformation on the basis of a complete NOE analysis. From the very small number of NOEs associated with the minor form that can be detected (only for Gln-81', Leu-6', and Lys-94'), it appears that the overall conformation is not significantly different from that of the major form, pointing to one or more highly localized conformational differences. Given the relatively slow rate of interconversion between the two forms, we can speculate that the chemical process responsible for the manifestation of the chemical exchange cross-peaks is a cis/trans peptide bond isomerization. We note that the estimated exchange rate for the chemical exchange process is on the high side of those measured for X-Pro cis/trans peptide bond isomerization in model peptides (Gratwohl & Wüthrich, 1981) and the calcium-binding protein calbindin (Chazin et al., 1989), but the lower estimate is comparable to that observed in Staphylococcal nuclease (Evans et al., 1989). In this respect it is interesting to point out that the residues to which chemical exchange cross-peaks have been assigned are clustered on one face of the X-ray structure of IL-1β, which includes portions of strands I and IV–VII. This part of the protein is rich in proline residues that appear close to the protein–solvent interface. These include Pro-78, Pro-87, Pro-91, and Pro-2.

Figure 8 also indicates another interesting aspect of the spectra of IL-1β that may relate to additional conformational heterogeneity of the protein. The diagonal peak of Phe-112, seen in Figure 8A, is considerably broader than most of the other amide NH signals, as judged by its much reduced height in comparison with the other resolved amide NH signals. Analysis of the Phe-112 intraresidue NH–C^αH HOHAHA and interresidue NH(Phe-112)–C^αH(Glu-111) NOESY

cross-peaks (Figure 8, parts C and B, respectively) suggests that the broad line shape arises from the amide NH resonance alone. Similarly, broad line shapes have been detected for the amide NH resonances of residues Ile-143, Thr-144, and Thr-124. These unusually large NH line widths can clearly be seen in the reduced heights and broad nature of the corresponding peaks in a double INEPT ¹⁵N–¹H Overbordenhausen experiment. The cross-peaks of the above four residues display this characteristic regardless of experimental conditions and in all the IL-1β protein samples we have studied, including wild-type, des-[Ala-1], K27C-, K93A-, and K94A-IL-1β. Phe-112 and Thr-124 possess amide NH resonances that exchange with solvent quite slowly in the presence of D₂O (Figures 3 and 4). It is therefore possible to eliminate solvent exchange broadening as a possible cause for the large line widths, at least in these two instances, which points to a conformational exchange process as the cause of the broad nature of these resonances. Interestingly, all four residues are grouped together in the three-dimensional X-ray structure at the junction between strands IX, X, and XII. It thus appears that the conformational difference has a highly localized effect on the protein structure. At this stage of the investigation, however, it is not possible to further elucidate the precise cause.

Concluding Remarks. We have described in detail an analysis of the secondary structure of recombinant IL-1β, based on a combination of short-, medium-, and long-range NOE analysis, and accurate ³J_{NHα} coupling constant and amide NH exchange rate measurements. With a molecular mass of 17.4 kDa and 153 amino acid residues, IL-1β is of a size that previously might have been thought to be inaccessible to such investigation by conventional ¹H 2D NMR spectroscopy. The basis for overcoming the obstacle of spectral complexity has been random ¹⁵N-isotope labeling of the protein in combination with "reverse" ¹⁵N–¹H correlation experiments that take advantage of the altered chemical shift dispersion of the ¹⁵N resonances, thereby affording effectively complete resolution of the backbone amide resonances. Three-dimensional heteronuclear NMR pulse sequences based on these experiments (i.e., 3D NOESY–HMQC and 3D HOHAHA–HMQC) enabled an almost complete analysis of the amide NH region of the ¹H NOESY spectrum of the protein. Additionally, the HMQC–J spectrum used for the measurement of ³J_{NHα} coupling constants and the ¹⁵N–¹H inverse correlation experiments used for the NH exchange rate measurements also make use of the separation of resonances on the basis of ¹⁵N chemical shift. The experience with IL-1β reported here, suggests that ¹⁵N labeling should be regarded as a priority for three-dimensional structure studies of any protein with molecular mass greater than ~15 kDa by NMR spectroscopy.

The secondary structure of IL-1β has been shown to comprise 12 β-strands combined in an extended antiparallel β-sheet arrangement. The indications are that this sheet is highly twisted in the three-dimensional fold of the protein. The strands are joined by a series of tight turns, short loops, and long loops that exhibit an approximate pseudo-three-fold symmetry. This picture of the structure of IL-1β is generally consistent with that of a recently reported unrefined three-dimensional structure of the protein determined by X-ray crystallography (Priestle et al., 1988). The close agreement between the results of the X-ray study and the NMR investigation reported here not only reinforces the NMR resonance assignments obtained previously, but also confirms the applicability of NMR spectroscopy as a tool for the investigation of the structure of proteins with molecular mass greater than 15 kDa. The current study provides a basis for the deter-

mination of the full three-dimensional solution structure of IL-1 β based on a complete analysis of all NMR parameters, as well as for studies of protein backbone dynamics, both currently being carried out in our laboratory.

ACKNOWLEDGMENTS

We thank Dr. Alan Shaw (Glaxo) for the construction of mutants reported in this paper, and Drs. Ad Bax, Dominique Marion, Lewis Kay, and Mitsuhiko Ikura for many useful discussions.

REFERENCES

- Aue, W. P., Bartholdi, E., Ernst, R. R. (1976) *J. Chem. Phys.* **64**, 2229–2246.
- Auron, P. E., Webb, A. C., Rosenwasser, J. J., Mucci, S. F., Rich, A., Wolff, S. M., & Dinarello, C. A. (1984) *Proc. Natl. Acad. Sci. U.S.A.* **81**, 7901–7911.
- Bax, A. (1989) *Methods Enzymol.* **176**, 151–168.
- Bax, A., Sklenar, V., Clore, G. M., & Gronenborn, A. M. (1987) *J. Am. Chem. Soc.* **109**, 7188–7190.
- Bax, A., Ikura, M., Kay, L. E., Torchia, D. A., & Tschudin, R. (1990) *J. Magn. Reson.* **86**, 304–318.
- Bodenhausen, G., & Ruben, D. J. (1980) *Chem. Phys. Lett.* **69**, 185–189.
- Braunschweiler, L., & Ernst, R. R. (1983) *J. Magn. Reson.* **53**, 521–528.
- Brown, S. C., Weber, P. L., & Mueller, L. (1987) *J. Magn. Reson.* **77**, 166–169.
- Chazin, W. J., Kördel, J., Drakenberg, T., Thulin, E., Brodin, P., Grundström, T., & Forsén, S. (1989) *Proc. Natl. Acad. Sci. U.S.A.* **86**, 2195–2198.
- Clore, G. M., & Gronenborn, A. M. (1987) *Protein Eng.* **1**, 275–288.
- Clore, G. M., & Gronenborn, A. M. (1989) *CRC Crit. Rev. Biochem. Mol. Biol.* **24**, 479–564.
- Clore, G. M., Bax, A., Wingfield, P. T., & Gronenborn, A. M. (1988) *FEBS Lett.* **238**, 17–21.
- Craig, S., Schmeissner, U., Wingfield, P. T., & Pain, R. H. (1987) *Biochemistry* **26**, 3570–3576.
- David, D., & Bax, A. (1985) *J. Am. Chem. Soc.* **107**, 2820–2821.
- Dinarello, C. A. (1984) *Rev. Infect. Dis.* **6**, 51–95.
- Dinarello, C. A. (1988) *Ann. N. Y. Acad. Sci.* **546**, 122–132.
- Driscoll, P. C., Clore, G. M., Beress, L., & Gronenborn, A. M. (1989) *Biochemistry* **28**, 2178–2187.
- Driscoll, P. C., Clore, G. M., Marion, D., Wingfield, P. T., & Gronenborn, A. M. (1990) *Biochemistry* **29**, 3542–3556.
- Ernst, R. R., Bodenhausen, G., & Wokaun, A. (1987) *Principles of Nuclear Magnetic Resonance in One and Two Dimensions*, Clarendon Press, Oxford, U.K.
- Evans, P. A., Kautz, R. A., Fox, R. O., & Dobson, C. M. (1989) *Biochemistry* **28**, 362–370.
- Fesik, S. W., & Zuiderweg, E. R. P. (1988) *J. Magn. Reson.* **78**, 588–593.
- Fesik, S. W., Gampe, R. T., & Rockway, T. D. (1987) *J. Magn. Reson.* **74**, 366–371.
- Finzel, B. C., Clancy, L. L., Holland, D. R., Watenpugh, K. D., & Einspahr, H. M. (1989) *J. Mol. Biol.* **209**, 779–791.
- Forman-Kay, J. D., Gronenborn, A. M., Kay, L. E., Wingfield, P. T., & Clore, G. M. (1990) *Biochemistry* **29**, 1566–1572.
- Gratwohl, C., & Wüthrich, K. (1981) *Biopolymers*, **26**, 2623–2633.
- Gronenborn, A. M., Clore, G. M., Schmeissner, U., & Wingfield, P. T. (1986) *Eur. J. Biochem.* **161**, 37–43.
- Gronenborn, A. M., Wingfield, P. T., Schmeissner, U., & Clore, G. M. (1988) *FEBS Lett.* **231**, 135–138.
- Gronenborn, A. M., Bax, A., Wingfield, P. T., & Clore, G. M. (1989a) *FEBS Lett.* **243**, 93–98.
- Gronenborn, A. M., Wingfield, P. T., & Clore, G. M. (1989b) *Biochemistry* **28**, 5081–5089.
- Huang, J. J., Newton, R. C., Horuk, R., Matthew, J. B., Covington, M., Pezzella, K., & Lin, Y. (1987) *FEBS Lett.* **223**, 294–298.
- Ikura, I., Marion, D., Kay, L. E., Shih, H., Krinks, M., Klee, C. B., & Bax, A. (1990) *Biochem. Pharmacol.* (in press).
- Jeener, J., Meier, B. H., Bachman, P., & Ernst, R. R. (1979) *J. Chem. Phys.* **71**, 4546–4553.
- Karplus, M. (1963) *J. Amer. Chem. Soc.* **85**, 2870–2871.
- Kay, L. E., & Bax, A. (1990) *J. Magn. Reson.* **86**, 110–126.
- Kay, L. E., Marion, D., & Bax, A. (1989a) *J. Magn. Reson.* **83**, 72–84.
- Kay, L. E., Ikura, M., & Bax, A. (1989b) *J. Am. Chem. Soc.* **112**, 888–889.
- Kay, L. E., Torchia, D. A., & Bax, A. (1989c) *Biochemistry* **28**, 8972–8979.
- MacDonald, H. R., Wingfield, P. T., Schmeissner, U., Shaw, A., Clore, G. M., & Gronenborn, A. M. (1986) *FEBS Lett.* **290**, 295–298.
- Macura, S., Huang, Y., Suter, D., & Ernst, R. R. (1981) *J. Magn. Reson.* **43**, 259–281.
- March, C. J., Mosley, B., Larsen, A., Cerretti, D. B., Breadt, G., Price, V., Gillis, S., Henney, C. S., Kroheim, S. R., Grabstein, K., Conlon, P. J., Hopp, T. P., & Cosman, D. (1985) *Nature (London)* **315**, 641–647.
- Marion, D., & Wüthrich, K. (1983) *Biochem. Biophys. Res. Commun.* **113**, 967–974.
- Marion, D., & Bax, A. (1988) *J. Magn. Reson.* **80**, 528–533.
- Marion, D., Kay, L. E., Sparks, S. W., Torchia, D. A., & Bax, A. (1989a) *J. Am. Chem. Soc.* **111**, 1515–1517.
- Marion, D., Driscoll, P. C., Kay, L. E., Wingfield, P. T., Bax, A., Gronenborn, A. M., & Clore, G. M. (1989b) *Biochemistry* **28**, 6150–6156.
- Marion, D., Ikura, M., Tschudin, R., & Bax, A. (1989c) *J. Magn. Reson.* **85**, 393–399.
- McConnell, H. M. (1958) *J. Chem. Phys.* **28**, 430–434.
- McIntosh, L. P., & Dahlquist, F. W. (1990) *Q. Rev. Biophys.* (in press).
- McIntosh, L. P., Griffey, R. H., Muchmore, D. C., Nielson, C. P., Redfield, A. G., & Dahlquist, F. W. (1987a) *Proc. Natl. Acad. Sci. U.S.A.* **84**, 1244–1248.
- McIntosh, L. P., Dahlquist, F. W., & Redfield, A. G. (1987b) *J. Biomol. Struct. Dyn.* **5**, 21–34.
- Moore, M. A. S. (1989) *Immunol. Res.* **8**, 165–175.
- Mosley, B., Dower, S. K., Gillis, S., & Cosman, D. (1987) *Proc. Natl. Acad. Sci. U.S.A.* **84**, 4572–4576.
- Mueller, L. (1987) *J. Magn. Reson.* **72**, 191–196.
- Oh, B.-H., Westler, M. W., Darba, P., & Markley, J. L. (1988) *Science* **240**, 908–911.
- Oppenheim, J. J., Kovacs, E. J., Matsushima, K., & Durum, S. K. (1986) *Immunol. Today* **7**, 45–56.
- Pardi, A., Billeter, M., & Wüthrich, K. (1984) *J. Mol. Biol.* **180**, 741–751.
- Powell, M. J. D. (1965) *Comput. J.* **7**, 303–307.
- Priestle, J. P., Schär, H.-P., & Grütter, M. G. (1988) *EMBO J.* **7**, 339–343.
- Priestle, J. P., Schär, H.-P., & Grütter, M. G. (1989) *Proc. Natl. Acad. Sci. U.S.A.* **86**, 9667–9671.
- Richardson, J. S. (1981) *Adv. Protein Chem.* **34**, 167–339.
- Shaka, A. J., Barker, P. B., & Freeman, R. (1985) *J. Magn. Reson.* **64**, 547–552.

- Stockman, B. J., Westler, W. M., Mooberry, E. S., & Markley, J. L. (1988) *Biochemistry* 27, 136-142.
- Torchia, D. A., Sparks, S. W., & Bax, A. (1988) *Biochemistry* 27, 5135-5141.
- Torchia, D. A., Sparks, S. W., & Bax, A. (1989) *Biochemistry* 28, 5509-5524.
- Wingfield, P. T., Payton, M., Tavernier, J., Barnes, M., Shaw, A., Rose, K., Simona, M. G., Demaczuk, S., Williamson, K., & Dayer, J.-M. (1986) *Eur. J. Biochem.* 160, 491-497.
- Wingfield, P. T., Payton, M., Graber, P., Rose, K., Dayer, J.-M., Shaw, A., & Schmeissner, U. (1987a) *Eur. J. Biochem.* 165, 537-541.
- Wingfield, P. T., Mattaliano, R. J., MacDonald, H. R., Craig, S., Clore, G. M., Gronenborn, A. M., & Schmeissner, U. (1987b) *Protein Eng.* 1, 413-417.
- Wingfield, P. T., Graber, P., Movva, N. R., Clore, G. M., Gronenborn, A. M., & MacDonald, H. R. (1987c) *FEBS Lett* 215, 160-164.
- Wingfield, P. T., Graber, P., Shaw, A. R., Gronenborn, A. M., Clore, G. M., & MacDonald, H. R. (1989) *Eur. J. Biochem.* 179, 565-571.
- Wüthrich, K. (1986) *NMR of Proteins and Nucleic Acids*, Wiley, New York.
- Wüthrich, K., Billeter, M., & Braun, W. (1984) *J. Mol. Biol.* 180, 715-740.
- Zuiderweg, E. R. P., & Fesik, S. W. (1989) *Biochemistry* 28, 2387-2391.

Accuracy of the *EcoRI* Restriction Endonuclease: Binding and Cleavage Studies with Oligodeoxynucleotide Substrates Containing Degenerate Recognition Sequences[†]

Vera Thielking, Jürgen Alves, Anja Fliess, Günter Maass, and Alfred Pingoud*

Zentrum Biochemie, Medizinische Hochschule Hannover, Konstanty-Gutschow-Strasse 8, D-3000 Hannover 61, West Germany

Received November 3, 1989; Revised Manuscript Received January 9, 1990

ABSTRACT: We have synthesized a series of 18 nonpalindromic oligodeoxynucleotides that carry all possible base changes within the recognition sequence of *EcoRI*. These single strands can be combined with their complementary single strands to obtain all possible *EcoRI** sequences (left), or they can be combined with a single strand containing the canonical sequence to obtain double strands with all possible mismatches within the recognition sequence (right):

GCGC A A A T T C CGCG

GCGC A A A T T C CGCG

CGCG T T T A A G GCGC

CGCG C T T A A G GCGC

The rate of phosphodiester bond cleavage of these oligodeoxynucleotides by *EcoRI* was determined in single-turnover experiments under normal buffer conditions in order to find out to what extent the canonical recognition site can be distorted and yet serve as a substrate for *EcoRI*. Our results show that oligodeoxynucleotides containing mismatch base pairs are in general more readily attacked by *EcoRI* than oligodeoxynucleotides containing *EcoRI** sites and that the rates of cleavage of the two complementary strands of degenerate oligodeoxynucleotides are quite different. We have also determined the affinities of these oligodeoxynucleotides to *EcoRI*. They are higher for oligodeoxynucleotides carrying a mismatch within the *EcoRI* recognition site than for oligodeoxynucleotides containing an *EcoRI** site but otherwise do not correlate with the rate with which these oligodeoxynucleotides are cleaved by *EcoRI*. Our results allow details to be given for the probability of *EcoRI* making mistakes in cleaving DNA not only in its recognition sequence but also in sequences closely related to it. Due to the fact that the rates of cleavage in the two strands of a degenerate sequence generally are widely different, these mistakes are most likely not occurring in vivo, since nicked intermediates can be repaired by DNA ligase.

Type II restriction endonucleases are considered to be part of a defense system that protects bacterial cells against foreign DNA, in particular bacteriophage DNA (Smith, 1979). They operate by recognizing a defined DNA sequence and cleaving the DNA within this sequence, thereby inactivating it. They do not attack the chromosomal DNA, provided it is kept in a methylated state by a companion modification enzyme.

Restriction endonucleases must be highly specific for their recognition sequence, since cleavage of the chromosomal DNA in other sequences not protected by methylation presumably is deleterious for the bacterial cell, as can be inferred from the observation that bacterial cells producing a restriction endonuclease are generally not viable in the absence of the corresponding modification enzyme [for review, cf. Wells et al. (1981), Malcolm (1981), Modrich and Roberts (1982), and Bennett and Halford (1989)].

Considerable progress has been made in understanding the molecular basis of the specificity of restriction enzymes, mainly due to chemical modification studies, in which the structural

[†] This work has been supported by grants from the Deutsche Forschungsgemeinschaft (Pi 122/2-3 and Ma 465/11-5) and the Fonds der Chemischen Industrie.

* To whom correspondence should be addressed.